Effect of Branch Distribution on Rheology of LLDPE during Early Stages of Crystallization

M. Y. Gelfer and H. H. Winter*

Department of Polymer Science and Engineering, University of Massachusetts, Amherst, Massachusetts 01003

Received April 15, 1999; Revised Manuscript Received October 8, 1999

ABSTRACT: For a series of semicrystalline ethylene−α-olefin copolymers (linear low-density polyethylene, LLDPE) produced by metallocene and Ziegler−Natta polymerization, the effect of the copolymer composition on the morphology and the evolution of linear viscoelastic properties during isothermal crystallization was studied. The purpose of this study is to explore the extreme sensitivity of rheology and processing to small variations in molecular detail in LLDPE. The metallocene LLDPE sample contains fewer branched units (2.6 mol % C-6) than the Ziegler−Natta copolymer (3.8 mol % C-6), but still, it melts at lower temperatures than the more branched Ziegler−Natta LLDPE analogue. Physical gelation as observed by rheology occurs over a broader temperature region for the metallocene LLDPE than for the Ziegler−Natta copolymer. DSC and rheological observations indicate that the solidification behavior in LLDPEs is determined more by the composition distribution than by the overall content of branched units. A HDPE was included in the study for comparison purposes.

Introduction

The evolution of mechanical properties during polymer crystallization is influenced not only by the bulk crystallinity but also by the size and functionality of the physical cross-links formed by the crystallites. It was shown that the transition from fluidlike to solidlike behavior occurs at the very early stages of crystallization, when the degree of crystallinity is well below 2 wt %.[1,2] Therefore, the early stages of crystallization are of primary importance for the development of morphology in the crystallizing polymer.

Linear low-density polyethylene (LLDPE) from Ziegler−Natta polymerization is highly heterogeneous[3,4] with broadly varying branch distributions. LLDPEs can be considered as blends of ethylene copolymers with variable branch contents. Literature data,[5] TREF information supplied by manufacturer, and our "DSC fractionation" results shown below suggest that, while metallocene LLDPEs were designed to have narrower composition distributions, even these systems might be considered blends rather than uniformly branched copolymers. Thus, LLDPEs melt over a rather broad temperature interval; their bulk rate of crystallization is determined by the superposition of crystallization rates of individual components weighted by their relative contents. In this study we apply DSC and time-resolved rheology techniques[1,6] to determine the effect of composition distribution in various metallocene and Ziegler−Natta LLDPEs on their linear viscoelastic behavior during crystallization. The major purpose of this investigation is to find the connections between copolymer composition, viscoelastic behavior of the polymer melt during crystallization, morphology, and the molecular mobility in the solid state.

Background Information

Uniform and Nonuniform Branching in LLDPEs. Commercial LLDPEs possess both intra- and intermolecular composition heterogeneity. In comparison, the ideal case of a uniformly branched copolymer would require that all molecules have the same relative content of branched units (no intermolecular composition heterogeneity) and that all distances between branches within molecules be the same (no intramolecular composition heterogeneity).

Let us first consider the behavior of *uniformly* branched copolymers. Numerous studies indicate that, during isothermal crystallization of LLDPE, short branches containing from 3 to 10 carbon atoms are excluded from the crystalline phase into an amorphous region, and the lamellar stems are formed from linear chain segments.[7] The lengths of such linear segments cannot exceed the distance between branches. As a result, chains with shorter distances between branches (i.e., with higher content of branched units x) will crystallize at lower temperatures. For instance, a recently synthesized uniformly branched ethylene copolymer containing one methyl branch for every nine carbons sharply melts[8] at −2 °C, compared to 135 °C for the HDPE in this study.

The exclusion of branches from the crystalline phase limits the maximum possible lamellar thickness $l_{0,max}$, which cannot be exceeded by the uniformly branched copolymer under any temperature regime (i.e., long annealing). The equilibrium melting temperature $T^0_{m,LLDPE}$ for such system will be below the ideal value of the unbranched chains, T^∞_{HDPE}. For the uniformly branched chains containing x mol % of branched units, $l_{0,max}$ should be proportional to $1/x$. Moreover, for low branching, when the crystalline structure does not depend on copolymer content, there should exist a one-to-one dependence between the content of branched units and the maximal possible lamellar thickness. Assuming that, for LLDPEs with low branching, the heat of fusion ΔH_m and the surface energy γ do not differ much from those for HDPE, one can estimate the depression of the equilibrium melting temperature ΔT_m in the uniformly branched LLDPE compared to HDPE of similar molecular weight:

10.1021/ma990588y CCC: $18.00
Published on Web 12/04/1999

$$\Delta T_m = T^{\infty}_{HDPE} - T^{0}_{m,LLDPE} = \frac{2\gamma T^{\infty}_{HDPE}}{\Delta H_m \, l_{0,max}(x)} \quad (1)$$

Here $l_{0,max}(x)$ is the maximal possible lamellar thickness for copolymer chains containing x mol % of branched units. T^{∞}_{HDPE} is the corresponding equilibrium melting temperature of the infinite HDPE crystal. Information on the heat of fusion ΔH_m and surface energy γ of HDPE is available in the literature.[9−11] For instance, Basset et al.[10] determined $\gamma = 92 \times 10^{-3}$ J m^{-2} and $T^{\infty}_{HDPE} = 142$ °C. A value $\Delta H_m = 295.8$ J/g can be found in the *Physical Properties of Polymers Handbook*.[11]

For highly branched systems ($x > 6$ mol %) branching dependence of melting temperature becomes more complicated. In such systems values of ΔH_m and γ significantly deviate from those determined for HDPE. Moreover, in highly branched ethylene copolymers the type of crystallites changes from lamellar structures to bundled crystals.[12]

Nonuniformity in inter- and intramolecular branching distributions causes the melting behavior in commercial LLDPEs to deviate from the one described by eq 1. Obviously, blockiness (the tendency of branched units to cluster rather than distributing randomly along the chain and between molecules) would strongly change the dependence between average lamellar thickness and copolymer composition. However, thorough investigations of both intermolecular and intramolecular distributions of short-chain branches using ^{13}C NMR and fractionation techniques never confirmed the presence of blocks formed by branched units.[12−15] Therefore, a high melting temperature for the subfractions of commercial LLDPE is the reliable indication of a low branching content.[16]

The more branched the polymer chain is, the less it can contribute to the crystalline phase. Because of the exclusion of branches from the crystalline region and the decrease in the crystallization rate due to branching, we conclude that the amorphous regions in semicrystalline LLDPEs should be enriched by more branched chains and the crystallites by more linear chain segments. Time-resolved WAXD and SAXS experiments showed[17] that, at low undercooling, the morphology development during crystallization of LLDPEs starts by the formation of thick primary lamellae from the longest linear chain segments. Then, the volume between primary lamellae is filled by thinner, less perfect crystals. As the branching increases, linear chain segments which are able to fit into the crystalline lattice become shorter, and the crystallization rate at given supercooling decreases.

Lambert and Phillips[18] used fractionated ethylene−α-olefin copolymers with very narrow composition distribution to show that the bulk crystallization rate is far slower for branched systems than for linear analogues of similar molecular weight at the same degree of supercooling. Obviously, faster crystallizing, less branched molecules can contribute the most to the thicker lamellae, hereby determining the properties of the crystalline phase at low degrees of crystallinity near the liquid-to-solid transition. Hence, for the least branched fraction of LLDPE, which would crystallize first under all temperature regimes, the branching distribution should have a major influence on the system properties near the liquid-to-solid transition and on the morphology of a semicrystalline copolymer.

DSC Fractionation. Exclusion of branches and significant difference in crystallization rate for systems with varying content of branched units creates opportunities for DSC analysis of composition distribution in a semicrystalline copolymer. The so-called "DSC fractionation" technique applies stepwise decreasing temperatures with $T_1 > T_2 \gg T_i > T_{i+1}$. The sample is being held isothermally at each T_i for some time t_h (in this study 100 min). After completion of these isothermal steps, the sample is rapidly cooled to −2 °C. Then, the sample is heated at a high rate (10 K/min) to record the thermogram. When treated according to this $T(t)$ protocol, a heterogeneous copolymer, containing chains with varying branching, will crystallize stepwise. During the first step, crystallites presumably only form by chains whose $T_m^0(x)$ exceeds T_i . Cocrystallization (i.e., inclusion of lower melting fractions) is assumed to be insignificant for the isothermal process, and provided the temperature is held long enough, the whole copolymer fraction satisfying the condition $T_m^0(x) > T_1$ will crystallize at this first step. Then, as the temperature is decreased from T_1 to T_2, more highly branched chains can crystallize, having lower crystallization temperatures $T_1 > T_m^0(x) > T_2$. The process repeats itself during the following sequence of temperature steps.

The chains with the highest content of branches crystallize during the final cooling scan or do not crystallize at all. The thermogram recorded at the final heating scan contains few melting peaks. The area of the ith peak (i.e., ΔH_i) corresponds to the total content of copolymers whose melting temperatures T_m^0 are above T_i but below T_{i+1}. The content of branched units x in these copolymers have to satisfy the condition $x_{i-1} < x < x_i$, where x_i is the content of branched units in the uniformly branched copolymer having T_m^0 equal to T_i.

DSC fractionation techniques allow separate observation of melting behavior of individually crystallizable subfractions. The method applies to bulk polymers without interference from any solvent. Crystalline subfractions are being distinguished on the basis of their lamellar thickness rather than on their average compositions. Hence, the exact form of melting temperature−composition relations is a measure of both inter- and intramolecular composition distributions in the polymer.

Because in this study we intend to characterize individual fractions in tested LLDPEs on the basis of their crystallization behavior rather than to determine their branching contents, we did not use any calibration curves or equations relating the branching distribution to the melting temperatures.

Physical Gelation by Crystallization A critical gel appears during a process of random linking of molecules into larger and larger clusters. The critical gel is a common boundary of liquid and solid regimes. No matter what objects are linked, they always exhibit a critical gel point if the system is disordered and linking processes are mainly random. At the critical point the system behaves neither as liquid nor as solid; its state can be characterized as critical gel. There are several theories describing critical gels, but they use the common preposition that the critical gel is self-similar. Self-similarity means that the structure of the critical cluster has no dominant length scale: there are holes at all lengths scales and connected strands at all lengths scales.[19]

Table 1. Samples of Ethylene−α-Olefin Copolymers

name	type	process	branching	properties
M1	LLDPE	metallocene	2.6 mol % C-6	M_w = 106749 g/mol M_w/M_n = 2.39 T_m(as is) = 119.1 °C
ZN1	LLDPE	Ziegler−Natta	3.8 mol % C-6	M_w = 115278 g/mol M_w/M_n = 3.96 T_m(as is) = 127.6 °C
MHD HDPE	metallocene	0		M_x = 110 000 g/mol T_m(as is) = 134.8 °C
M2	highly branched PE	metallocene	11 mol % C-4	T_m = 55−60 °C

The gelation process is most clearly defined for chemical gelation where molecules are linked by covalent bonds. The approach of the gel point by the gelling system has typically been recognized by a zero-shear viscosity η_0 which increases during cross-linking until it diverges at the gel point. Beyond the gel point the material can be characterized by its growing equilibrium modulus, G_e, which is zero before and at the gel point. It was shown that the chemical gel point has its own distinct rheological properties, which is characterized by slow power-law dynamics. This expresses itself in a self-similar relaxation modulus[20,21]

$$G(t) = S_c t^{-n_c}; \quad \text{for } \lambda_0 < t < \infty \tag{2}$$

The gel stiffness, S_c [Pa s^n], and the critical relaxation exponent, n_c[−], are rheological material parameters; n_c can adopt values $0 < n_c < 1$. The self-similar relaxation occurs in the terminal zone at long times, $\lambda_0 < t < \infty$. The lower limiting relaxation time λ_0 characterizes the crossover to the entanglement relaxation or glass transition. The self-similar relaxation behavior can also be expressed by a power law relaxation time spectrum (CW spectrum[20])

$$H(\lambda) = \frac{S_c \lambda^{-n_c}}{\Gamma(n_c)}; \quad \text{for } \lambda_0 < \lambda < \infty \tag{3}$$

$\Gamma(y)$ is the gamma function. The self-similar relaxation results in power-law dynamic moduli

$$G'(\omega) = S_c \Gamma(1 - n_c) \cos(n_c \pi/2) \omega^{n_c}$$

$$G''(\omega) = S_c \Gamma(1 - n_c) \sin(n_c \pi/2) \omega^{n_c} \quad \text{for } \omega < 1/\lambda_0 \tag{4}$$

and a constant loss angle $\delta = \pi n_c/2$ at low frequencies. This dominance of self-similar mechanical properties will be used to detect the gel point in this study. As larger and larger self-similar clusters are being formed, the correlation length, ξ, increases. At the percolation threshold, self-similar clusters extend over the whole sample (ξ diverges). This marks the critical gel point. As cross-linking density increases further, the material's behavior changes to solidlike, and the size of unconnected regions decreases.[19]

Recently, it was shown that for semicrystalline polymers the evolution of viscoelastic behavior during the early stages of crystallization closely resembles chemical gelation process.[1,2,20,22,23] It was proposed that early stages of crystallization could be viewed as physical gelation, where crystallites act as the physical cross-links, linking molecular chains together. It is known[24] that the same polymer chain can go through several amorphous and crystalline regions. Thus, crystalline regions can be presented as cross-links, linking together several neighboring chains. Chains protrude from the crystalline regions, so their segments remaining in the amorphous phase are mobile. Therefore, random linking of macromolecules does occur during crystallization processes.

An important feature of physical cross-linking by crystallization is that crystallites acting as physical cross-links are significantly larger than covalent chemical bonds. Indeed, the C−C bond length is 0.15 nm. The average lamellar thickness l_{avg} in tested polymers was estimated on the basis of the melting temperature using the well-known Gibbs−Thomson equation.[11] According to our evaluation, the maximal lamellar thickness to be expected in ethylene copolymers crystallized at the experimental conditions of this study could not exceed 30 nm. However, the extended length of an all-trans linear PE chain of M_w = 100 000 can be estimated as 200 nm; i.e., the single chain is long enough to pass through several crystalline domains, acting as physical cross-links. Here, it has to be kept in mind that the lamellar thickness and therefore the size of physical cross-links are strongly influenced by the thermal history and copolymer composition.

Another significant factor complicating the interpretation of experimental results is the possibility of liquid−liquid phase separation in LLDPE melts at temperatures above T_m. On the basis of SANS, SAXS, and SEM data,[25−29] it was proposed that liquid−liquid phase separation can be observed in molten blends of HDPE and LDPE and in the melt of highly heterogeneous LLDPEs with highly branched fractions ($x > 8$ mol %). Still, the precise degree of composition heterogeneity required for liquid−liquid phase separation remains undetermined. In the following we assume that for tested LLDPE melts crystallization has far greater influence on the viscoelastic properties than liquid−liquid phase separation.

The exclusion of branched units from the crystalline phase leads to a composition segregation during crystallization, when chains with different branch contents form separate crystalline structures rather than cocrystallize.[30,31] These phenomena are expected to affect the rheological behavior during crystallization and the morphology of the crystallized copolymer. The complete theory of physical gelation accounting for these phenomena has yet to be developed.

This study concentrates on early stages of crystallization at low ΔT where the fractions of polymer, which can crystallize, depend on the branch content.

Experimental Section

Four samples (Table 1) were chosen to specifically find composition−texture relations. The ethylene copolymers tested were selected to represent different types of composition distribution, occurring in industrial ethylene−α-olefin systems. LLDPE samples M1 and ZN1 used in this study were characterized by TREF (temperature raising elution fractionation)

at Exxon. TREF efficiency for LLDPEs characterization is well established by numerous studies.[3−5] TREF results confirm that the composition distribution for M1 is typical for metallocene LLDPEs, while composition of ZN1 is representative for Ziegler−Natta systems. M1 contains a variety of subfractions with branching varying from 0.9 to 9 mol %. Contents of branched units in subfractions of ZN1 varied from 0.5 to 11 mol %.

HDPE (MHD) and highly branched ethylene−butene copolymer (M2) containing 28 mol % C-4 units were manufactured at Exxon by metallocene polymerization. M2 and MHD were tested for comparison purposes in order to elucidate the effect of branching on crystallization behavior.

In addition to TREF, the "DSC fractionation" technique[5,16,32−34] was utilized for studying the composition distribution in the ethylene copolymers. DSC experiments were performed on a DSC 2910 scanning calorimeter (TA Instruments).

Oscillatory shear experiments on a strain controlled rheometer ARES LS 3 (Rheometric Scientific) with 25 mm parallel plates used frequencies of 0.1−100 rad/s. While such a frequency range allowed for the observation of the low-frequency "power law region" of G', G'' vs ω, the measuring time necessary to obtain single data points was short enough, so that the rheological properties of crystallizing sample did not undergo significant change during individual measurements. A small strain amplitude of $\gamma_a = 0.01$ was chosen in order to ensure minimal influence of imposed strain on the crystallization process. Rheological experiments started out by melting of a sample at 160 °C for 30 min. Then, the sample was rapidly cooled to the desired experimental temperature, T_{exp}, and held there for crystallization studies. All rheological tests were performed in inert atmosphere, under the flow of nitrogen.

Experimental Results and Discussion

DSC melting experiments (Figure 1) compare samples that were rapidly quenched in water (curves I) and samples that were stepwise crystallized according to the DSC fractionation technique (curves II). We start with conventional Ziegler−Natta (ZN1) LLDPE. The pronounced peak at 127.5 °C of the DSC thermogram in (Figure 1a, curve II) indicates that the major component in the crystalline fraction in ZN1 is formed by copolymer with long linear segments (low branching) whose measured melting temperature $T_{m,eff}$ does not differ much from that of HDPE ($T_{m,eff,HDPE}$ = 134.5 °C; Figure 1b, curve I). The low intensity of peak 2 (Figure 1a, curve II) indicates that the content of more branched chains in the crystalline phase of conventional LLDPE is small. Peak 3, whose melting temperature (109.2 °C) is below the lowest temperature of isothermal crystallization (112 °C), corresponds to the crystalline subfraction formed during the final cooling scan.

No peak splitting occurs upon DSC fractionation of metallocene HDPE MHD (Figure 1b, curves I and II), proving the connection between peak splitting and composition heterogeneity. MHD is the reference polymer for our studies.

In contrast to ZN1, the corresponding thermogram for metallocene LLDPE M1 (Figure 1c, curve II) contains three peaks (1−3) of comparable intensity formed during isothermal "steps" and peak 4 corresponding to polymer the subfraction crystallized during the final cooling scan. Similar area of peaks 1−3 suggests about equal amounts of corresponding crystalline subfractions. Despite the lower overall branching in M1 (as compared to ZN1), the highest melting subfraction 1 in M1 still melts at 123.2 °C, below 127.5 °C, which was found for the major crystalline subfraction in ZN1. This is a rather

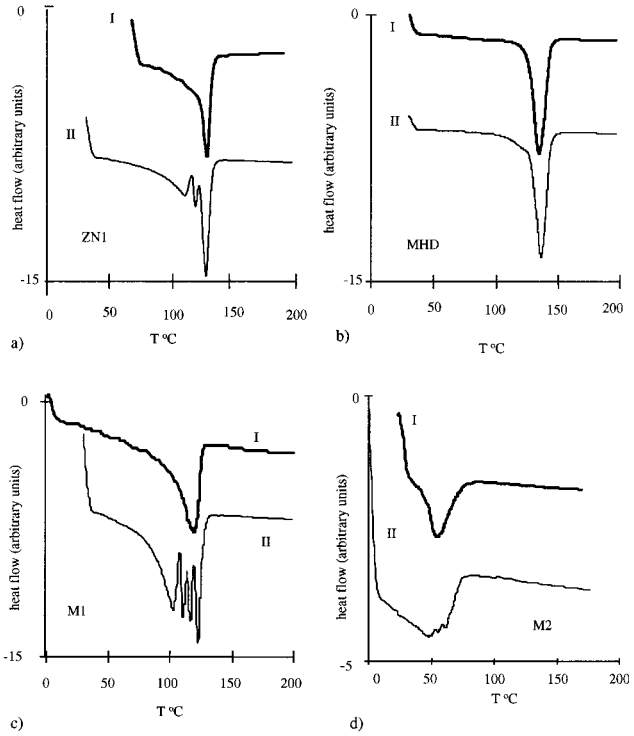

Figure 1. DSC fractionation of ethylene copolymers. Samples I had been rapidly quenched, and samples II had been step-crystallized. (a) Ziegler−Natta LLDPE ZN1. Sample I with T_m = 127.5 °C and ΔH_{eff} = 120.6 J/g. Sample II was step-crystallized for 100 min each at 127, 122, 117, and 112 °C; the corresponding DSC peaks are at 127.5, 118.5, and 109 °C. The pronounced peak at 127.5 °C corresponds to the least branched crystalline subfraction. Peak 3 at 109 °C corresponds to the crystalline subfraction formed during final quenching scan. (b) Metallocene HDPE MHD. Sample I with T_m = 134.5 °C and ΔH_{eff} = 120.6 J/g. Sample II was step-crystallized for 100 min each at 135, 130, 125, and 120 °C; single peak at 136.5 °C. (c) Metallocene LLDPE M1. Sample I with T_m = 119.2 °C and ΔH_{eff} = 112.6 J/g. Sample II was step-crystallized for 100 min each at 119, 114, 109, and 104 °C; the corresponding DSC peaks observed at 123.2, 115.6, 110.7, and 102.7 °C. Similar intensity of peaks 1−3 proves broad composition distribution in the crystalline fraction of M1. Peak 4 at 102.7 °C corresponds to crystalline subfraction formed during final quenching scan. (d) Highly branched metallocene ethylene−α-olefin copolymer M2. Sample I with T_m = 54.1 °C and ΔH_{eff} = 34.5 J/g. Sample II was step-crystallized for 100 min each at 60.5, 50, and 45 °C; the corresponding DSC peaks observed at 61.5, 55.8, and 48.8 °C. The poor resolution of melting peaks can be attributed to the low crystallization rate in this highly branched PE copolymer.

surprising result which indicates that the branches are more evenly distributed in M1 than in ZN1. ZN1 must have a substantial fraction of molecules with long stems without branching and also a large fraction of molecules that are very highly branched (so that they can barely crystallize).

The thermogram for highly branched metallocene copolymer M2 (Figure 1d) includes three poorly resolved peaks of comparable intensity. Slow crystallization of M2 and significant supercooling required to observe it can be related to the high branching in this copolymer.[18]

Thus, the crystalline phase of metallocene copolymers M1 (Figure 1c, curve II) and M2 (Figure 1d, curve II) treated according to steplike temperature protocol contains a variety of subfractions with gradually changing content of branched units x.

TREF data (Figure 2) are in a good agreement with "DSC fractionation" results. TREF plot for M1 (Figure

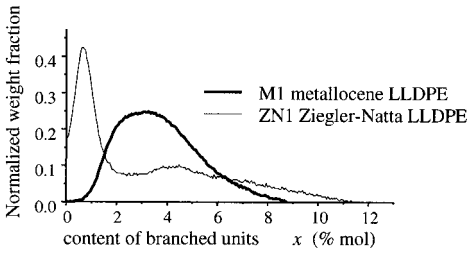

Figure 2. TREF data for Ziegler−Natta and metallocene LLDPEs, ZN1 and M1. Note the bimodal composition distribution and higher composition heterogeneity for ZN1. All plots are normalized for unit area. Data were supplied by Exxon Chemical.

2) can be described as single, rather broad peak with center at $x = 3.7$ mol %. In contrast to that, the composition distribution for ZN1 is distinctly bimodal. It contains an intense narrow peak with maximum at $x = 0.67$ mol % and a broad maximum centered at $x = 4.4$ mol %. Therefore, the intense high-temperature melting peak 1 of ZN1 (DSC thermogram of Figure 1a) belongs to a significant fraction of molecules that are rather narrowly distributed and practically without branches ($0 < x < 1$ mol %) as observed by TREF (Figure 2). In comparison, the higher branched subfractions in ZN1 ($4 < x < 11$ mol %) seem to crystallize during the final cooling step or not crystallize at all. Chains with intermediate branching ($2 < x < 4$ mol %) seem to be missing in ZN1. Indeed, the intensity of peak 2 in Figure 2a is far below that of peaks 1 and 3. TREF data prove that M1 contains comparable amounts of subfractions with branching content gradually changing from 2 to 6 mol %; this type of composition distribution results in similar intensity of peaks 1−3, observed in Figure 1c. Consequently, M1 melts over a wide temperature range and at a lower temperature than ZN1 despite its lower branching content.

The statistic character of intramolecular branching distribution creates the opportunity for the formation of both long and short methylene sequences within the same polymer chain.. Thus, in DSC fractionation, where physical separation of polymer chains does not occur, the same chain can contribute to few "factions". However, the observed agreement between DSC and TREF data indicates that the content of chains included in more than one subfraction with different equilibrium crystallization temperatures is rather small. Data of Deffieux et al.[16] indicate that during isothermal crystallization the extent of cocrystallization of chains with different branching is insignificant. Probably these phenomena can be related to steric factors. According to Akpalu et al.,[17] thick crystallites formed at a low degree of supercooling form the framework of supermolecular structures (spherulites). Further crystallization occurs within the space between thicker lamellae. Thus, if the molecule containing short and long methylene sequences is crystallized at low supercooling, longer segments will be able to form thick crystallites, while shorter methylene segments, unable to crystallize at given temperature, will remain in the amorphous domain. As temperature decreases, the mobility of shorter methylene sequences will be greatly reduced by attached crystalline regions, thus hindering cocrystallization with segments from other chains.

In that paper we were more concerned with crystallization behavior than with branching distribution itself, so while the question of fractionation unit in DSC and

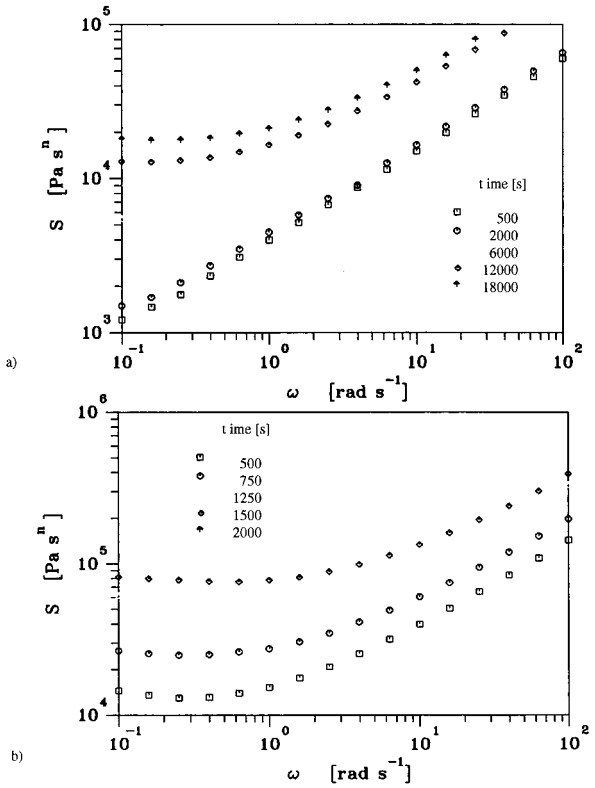

Figure 3. Change of $S'(\omega)$ with crystallization time for M1 metallocene LLDPE. (a) Crystallization at $T_{exp} = 122$ °C; "plateau region" can be observed for the frequency range 0.1−0.8 s^{-1} for $t > 12\,000$ s. $T^{\infty}_{HDPE} - T_{exp} = 20$ K. (b) Crystallization at $T_{exp} = 119$ °C; "plateau region" can be observed for the frequency range 0.1−1.0 s^{-1} for $t \geq 500$ s. The faster development of the "plateau region" in (b) shows how a higher crystallization rate at lower temperatures results in a rapid liquid-to-solid transition. $T^{\infty}_{HDPE} - T_{exp} = 23$ K with $T^{\infty}_{HDPE} = 142.0$ °C.

TREF techniques is important, it should not affect our conclusions.

Mechanical Spectroscopy. To follow the crystallization of LLDPEs by means of time-resolved rheometry, we will express the data with material functions[21]

$$n(\omega) = \frac{2}{\pi} \arctan \frac{G''(\omega)}{G'(\omega)} \tag{5}$$

$$S'(\omega) = \frac{G'(\omega)}{\Gamma(1 - n) \cos(n\pi/2)\omega^{-n}} \tag{6}$$

Both $n(\omega)$ and $S'(\omega)$ are combinations of measured variables. Indeed, n is the normalized phase angle, $2\delta/\pi$, and stiffness $S'(\omega)$ is a normalized storage modulus $G'(\omega)$. The solidification process causes a decrease in δ and an increase in G'. The gel point (GP) is special in the sense that both $n(\omega) = n_c$ and $S'(\omega) = S_c$ become material constants; i.e., they do not depend on frequency below some characteristic frequency, $\omega < 1/\lambda_0$. Note that the stiffness could also be defined with $G''(\omega)$, see eq 3; the data analysis would be similar. Preferably, one will use the G' definition for stiff materials (as in this study) and the G'' definition for softer gels.

$n(\omega)$ and $S'(\omega)$ are most suitable material functions for analyzing the time evolution of the solidification process in the vicinity of the gel point. In general, the phase angle $n(\omega)$ decreases and the stiffness $S'(\omega)$ increases during solidification. In addition, the appear-

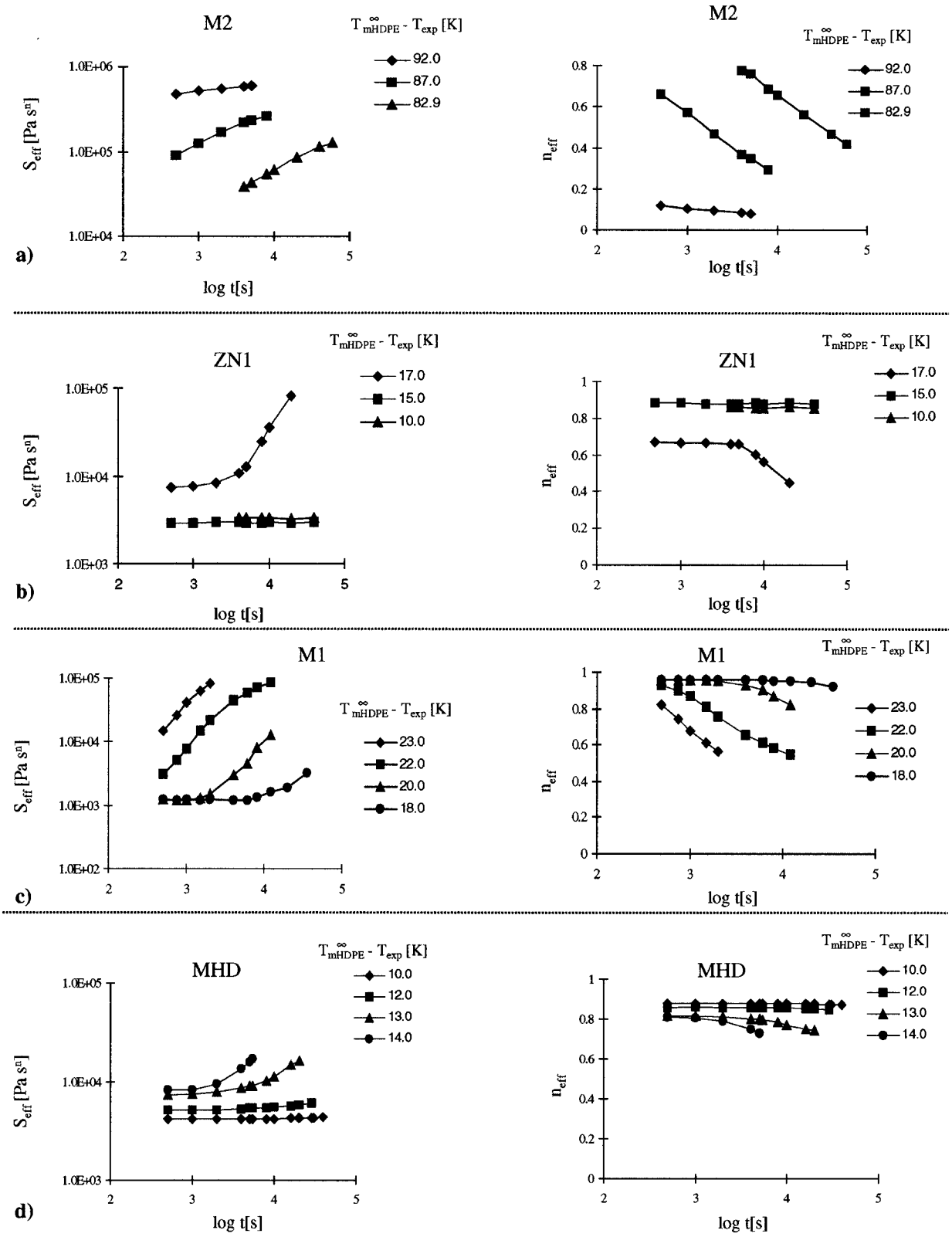

Figure 4. Evolution of $S'(\omega)$ and $n(\omega)$ with time during crystallization of ethylene copolymers. All S_{eff} denote $S'(\omega)$ values determined at $\omega = 0.1$ s^{-1}. Parameter is $\Delta T = T^{\infty}_{HDPE} - T_{exp}$, where we took $T^{\infty}_{HDPE} = 142.0$ °C. (a) Highly branched metallocene ethylene−α-olefin copolymer (M2); (b) Ziegler−Natta LLDPE (ZN1); (c) metallocene LLDPE (M1); (d) metallocene HDPE (MHD).

ance of a "plateau region", $S'(\omega) = S_c$, specifies the instant of liquid-to-solid transition. Stiffness $S'(\omega)$ [Pa s^n] is a more convenient parameter than G' or G'' for characterization of solidification behavior. During gelation, both viscosity and elasticity increase while $S'(\omega)$ accounts for both properties as indicated by its dimension [Pa s^n].

Figure 3 demonstrates the appearance of a low-frequency "plateau region" of $S'(\omega)$ measured during crystallization of M1. Similar "plateau regions" were observed for the majority of tested crystallizing systems. Because the measured melting temperatures of LLDPEs can be influenced by thermal history of the samples, the equilibrium melting temperature of the infinite HDPE

crystal, T^{∞}_{HDPE}, was used as a reference for specifying the degree of supercooling, $\Delta T = T^{\infty}_{HDPE} - T_{exp}$. Low-frequency values of $S'(\omega)$ and n are presented in Figure 4; these were measured at 0.1 s^{-1}, which in most cases lies within the plateau region (Figure 3).

It can be seen that a drastic difference exists between the solidification behavior of a conventional LLDPE (ZN1, Figure 4b) and metallocenes (M1, Figure 4c; M2, Figure 4a). Solidification of conventional LLDPE (Figure 4a) did not start until supercooling reached 17 K, and then rapid solidification occurred.

The reference metallocene HDPE (MHD) (Figure 4d) solidified only when the degree of supercooling reached 13 K; then the solidification rate quickly increased over a temperature range of 2 K.

For metallocene LLDPEs the behavior is quite different: a gradual increase in the solidification rates with the increase of ΔT was observed over the broad range of temperatures both for M1 (Figure 4c) and for M2 (Figure 4a). The gradual change in the solidification rate was observed over the temperature range exceeding 7 K for M1 and 10 K for M2. The slow crystallization of M2 and the significant supercooling required can be related to the very high branching in this copolymer.[18]

The observed drastic differences in the solidification behavior of Ziegler−Natta and metallocene LLDPEs are attributed to the difference in the branching distribution. As was shown by DSC fractionation (Figure 1), metallocene ethylene−α-olefin copolymers contain comparable amounts of subfractions with gradually varying branching contents. Thus, as the degree of supercooling increased, the involvement of more branched subfractions causes the gradual increase of the overall solidification rate (Figure 4a,c).

In comparison, conventional LLDPE (ZN1) did not solidify until the conditions for the crystallization of its major crystallizable fraction were reached, and then the sample solidified over a relatively narrow temperature range. In the Ziegler−Natta system, contents of other branched subfractions in the crystalline phase were relatively low, even for step-crystallized sample. Thus, the least branched fraction dominates the overall solidification process over the whole range of tested temperatures. The solidification behavior of HDPE (MHD) (Figure 4d) is quite similar to that of conventional LLDPE. For low supercooling, solidification was undetectable at the time scale of our experiment. As the critical degree of supercooling was reached, the significant increase in the solidification rate was observed over a narrow temperature interval (2 K), corresponding to the crystallization of HDPE.

Received results are in good agreement with data by Phillips et al.,[18] who observed that the range of crystallization temperatures is broader for metallocene than for Ziegler−Natta copolymers in both isothermal and nonisothermal experiments.

Conclusions

The effect of composition distribution in LLDPEs on their solidification behavior during crystallization has been studied. It was found that the type of composition distribution rather than the overall content of branched units determines the properties of these copolymers.

The general composition distribution may be broader for conventional LLDPE (ZN1) than for metallocene systems (M1, M2); however, as our DSC fractionation and rheological results indicate, it is a relatively narrow, highest melting, least branched subfraction of Ziegler−Natta LLDPE (ZN1) which contributes the most to the crystallization-induced solidification of this copolymer. It resulted in a narrower solidification interval for Ziegler−Natta system than for metallocene LLDPE. In contrast to ZN1, the solidification behavior of the metallocene copolymer M1 is determined by crystallization of many subfractions, able to contribute to the overall solidification process in the temperature interval chosen for the rheological experiments.

The ability to predict the structure and solidification behavior of LLDPE copolymers on the basis of their composition can be extremely useful for the optimization of materials and industrial processes. Indeed, copolymers and blends of copolymers with desired properties both in the melt and in the bulk state may be produced by blending or by varying the catalyst. These materials will deform and solidify in a desired way under the influence of stress, strain, and temperature fields occurring during processing.

Acknowledgment. We gratefully acknowledge the support of the Exxon Chemical Company, Baytown, TX and of NSF/MRSEC DMR 9625485. Dr. F. Chambon, Exxon, contributed with helpful discussions, with molecular characterization, and with TREF data. We are also grateful for helpful discussions with Prof. K. Schmidt-Rohr, Amherst.

References and Notes

(1) Schwittay, C.; Mours, M.; Winter, H. H. *Faraday Discuss.* **1995**, *101*, 93.
(2) Pogodina, N. V.; Winter, H. H. *Macromolecules* **1998**, *31*, 8164. Pogodina, N. V.; Siddiquee, S. K.; van Egmond, J. W.; Winter, H. H. *Macromolecules* **1999**, *32*, 1167.
(3) Mathot, V. B. F. In *Advances in Polyolefins;* Chung, T. C., Ed.; Plenum Press: New York, 1993; p 121.
(4) Mathot, V. B. F.; Pijpers, M. F. J. *J Appl. Polym. Sci.* **1990**, *39*, 979.
(5) Starck, P. *Polym. Int.* **1996**, *40*, 111.
(6) Mours, M.; Winter, H. H. *Rheol. Acta* **1994**, *33*, 385.
(7) Flory, P. J. *Trans. Faraday Soc.* **1955**, *51*, 848.
(8) Wagener, K. B.; Valenti, D.; Hahn, S. F. *Macromolecules* **1997**, *30*, 6688.
(9) Wunderlich, B. *Macromolecular Physics;* Academic Press: New York, 1980; Vol. 1.
(10) Bassett, D. C.; Hodge, A. M.; Olley, R. H. *Proc. R. Soc. London* **1981**, *A377*, 39.
(11) Mandelkern, L.; Alamo, R. G. In *Physical Properties of Polymers Handbook*; Mark, E. J., Ed.; American Institute of Physics: Woodbury, NY, 1996; p 123.
(12) Besanson, S.; Minick, J.; Moet, A.; Chum, S.; Hiltner, A.; Baer, E. *J. Polym. Sci., Phys.* **1996**, *34*, 1301.
(13) Hsieh, E. T.; Randall, J. C. *Macromolecules* **1982**, *15*, 353.
(14) Kimura, K.; Shigemura, T.; Yuasa, S. *J. Appl. Polym. Sci.* **1984**, *29*, 3161.
(15) Kimura, K.; Yuasa, S.; Maru, Y. *Polymer* **1984**, *25*, 441.
(16) Deffieux, A.; Ribeiro, M.; Adisson, E.; Fontanille, M. *Polymer* **1992**, *33*, 20, 4337.
(17) Akpalu, Y.; Hsiao, B. S.; Stein, R. S. Muthukumar, M. Private communication.
(18) Lambert, W. S.; Phillips, P. J. *Polymer* **1996**, *3*, 3585. Lambert, W. S.; Phillips, P. J. *Macromolecules* **1994**, *27*, 3537. Wagner, J.; Abu-Iqyas, S.; Monar, K.; Phillips, P. *J. Polymer* **1999**, *40*, 4717. Kim, M.-H.; Phillips, P. J. *J. Appl. Polym. Sci.* **1998**, *70*, 1893.
(19) Vilgis, T. A.; Hess, W.; Winter, H. H. *Macromolecules* **1988**, *21*, 2536.
(20) Chambon, F.; Winter, H. H. *Polym. Bull.* **1985**, *13*, 499. Winter, H. H.; Chambon, F. *J. Rheol.* **1986**, *30*, 367. Chambon, F.; Winter, H. H. *J. Rheol.* **1987**, *31*, 683.
(21) Winter, H. H.; Mours, M. *Adv. Polym. Sci.* **1997**, *134*, 165.

(22) Lin, Y. G.; Mallin, D. T.; Chien, J. C. W.; Winter, H. H. *Macromolecules* **1991**, *24*, 850.
(23) Nijenhuis, te K.; Winter, H. H. M*acromolecules* **1989**, *22*, 411.
(24) Young R. J.; Lovell P. A. *Introduction to Polymers*; Chapman & Hall: London, 1991; p 284.
(25) Alamo, R. G.; Graessley, W. W.; Krishnamoorti, R.; Loshe, D. J.; Londono, J. D.; Mandelkern, L.; Stehling, F. C.; Wignall, G. D. M*acromolecules* **1997**, *30*, 561. Alamo, R. G.; Graessley, W. W.; Krishnamoorti, R.; Loshe, D. J.; Londono, J. D.; Mandelkern, L.; Stehling, F. C.; Wignall, G. D. M*acromolecules* **1996**, *29*, 5332. Alamo, R. G.; Londono, J. D.; Mandelkern, L.; Stehling, F. C.; Wignall, G. D. *Macromolecules* **1994**, *27*, 411. Alamo, R. G.; Wignall, G. D.; Londono, J. D.; Lin, J. S.; Galante, M. J.; Mandelkern, L. *Macromolecules* **1995**, *28*, 3156.
(26) Barham, P. J.; Hill, M. J.; Keller, A. *Polymer* **1992**, *33*, 2530.
(27) Mumby S. J.; vanRuiten, J. *Polymer* **1995**, *36*, 2921.
(28) Nesarikar, A.; Crist, B.; Davidovich, A. *J. Polym. Sci., Part B: Polym. Phys.* **1994**, *32*, 641.
(29) Crist, B.; Hill, M. *J. Polym. Sci., Part B: Polym. Phys.* **1991**, *35*, 2329.
(30) Cheng, Z. D.; Fu, Q.; Chiou, F.-C.; McCreight, K. W.; Guo, M.; Tseng, W. W. *J. Macromol Sci., Phys.* **1997**, *36*, 41.
(31) Groenickx, G.; Defoor, F.; Reynaers, H.; Schouterden, P.; Heijden, Van der, B. *J. Appl. Polym. Sci.* **1993**, *47*, 1839.
(32) Groenickx, G.; Schouterden, P.; Heijden, Van der B.; Jansen, F. *Polymer* **1987**, *28*, 2099.
(33) Keating, M. Y.; McCord, E. F. *Thermochim. Acta* **1994**, *243*, 129.
(34) Balbontin, G.; Camurati, I.; Dall'Occo, T.; Finotti, A.; Franzese, R.; Vecellio, G. *Angew. Macromol. Chem.* **1994**, *219*, 139.

MA990588Y